IOP Conference Series: Earth and Environmental Science

PAPER • OPEN ACCESS

Experimental and numerical investigation of flows inside draft tube of a pump-turbine

To cite this article: X D Lai *et al* 2019 *IOP Conf. Ser.: Earth Environ. Sci.* **240** 072044

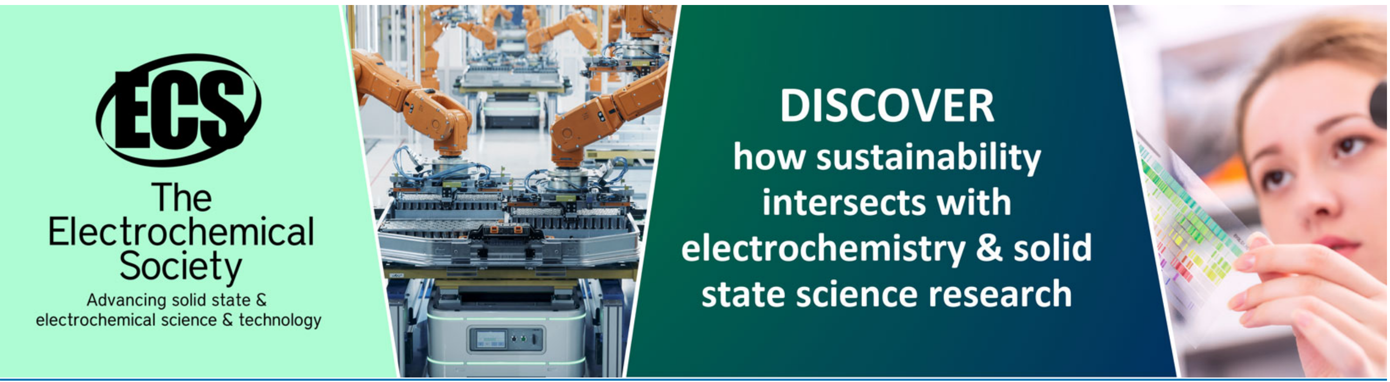

Experimental and numerical investigation of flows inside draft tube of a pump-turbine

X D Lai[1,2], Q W Liang[3], D X Ye[2], X M Chen[1], Q Q Gou[1] and Q H Zhang[1]
[1] School of Energy and Power Engineering, Xihua University, Chengdu, Sichuan, China
[2] Key Laboratory of Fluid and Power Machinery, Ministry of Education (Xihua University), Chengdu, China
[3] Dongfang Electric Machinery Co. Ltd, Deyang, China

corresponding author's e-mail: laixd@mail.xhu.edu.cn

Abstract. To determine the flow patterns and validate the flow simulation inside a pump-turbine, Laser Doppler Velocimetry (LDV) measurements and 3D flow simulation in the draft tube of a high-head pump-turbine have been performed at normal operating conditions in turbine and pump modes. Velocity distributions were measured for operating conditions corresponding to the rated head H=600m and the optimum head H=750m at turbine mode for various loads ranging from 40% to 120% of the rated power. The 3D flows through the full pump-turbine model have also been investigated with numerical simulations at all the measured operating points. Both measured and simulated velocity profiles are presented and analyzed to show the influence of operating parameters on the velocity and vortex characteristics in draft tube. Comparison of the measurement and simulation results shows rather good agreement in the vortex-free zone but clear discrepancies at part loads far from BEP. The experimental data such as the velocity profiles, vortex ropes visualization and frequency characteristics of the instantaneous tangential velocity at typical operating points are used to validate the precision of the model and method in the numerical simulation. The presented methodology and techniques in this paper have been demonstrated very helpful in R&D of pump-turbines at two Pumped storage Power plants in China.

1. Introduction

To provide a rapid adjustment to the electricity grid, pump-turbines are subject of quick switching between pumping and generating modes and to extend operation at off-design conditions [1]. Due to the continuously increasing requirements of wide operating capability, to accurately analyze and predict the unsteady flows in draft tube has become more and more important in the process of design as well as in the operation of an existed pump-turbine. Although numerical flow simulations are widely applied to investigate flow structures inside hydraulic machines [1-6], as the flow has a strong swirling component in part load operation, it is still difficult to accurately predict the flows and in particular the flows inside draft tube [2]. The main objectives of this investigation were to reliably determine the structure of the flow in the draft tube of a high-head pump-turbine model, as well as to obtain experimental data to verify the model and method of numerical simulation. To achieve this goal, the axial and the tangential velocities measurements with Laser Doppler Velocimetry (LDV) was required to conduct on a high precision commercial hydraulic machinery test stand at typical operating points under turbine and pump modes. Although some recent investigations with LDV have been carried out in the turbine [7-9], which show significant works on this issue, it is still a great challenge task to measure the flow field in the draft tube of a Francis pump-turbine model at different operating points under turbine and pump modes. This paper shows the results of LDV velocity measurement inside the draft tube cone of a Francis pump-turbine with the head up to H=750m. Measurements were taken for typical operating points covering the speed factor n_{ED}=0.21 and n_{ED}=0.19 for various loads ranging from 40% to 120% of the rated power at turbine mode, and also for operating at minimum head/maximum discharge and maximum head/minimum discharge corresponding to the prototype at pump mode. Meanwhile, the 3D flows through the completed pump-turbine model were numerically simulated with ANSYS/CFX® software at all the measured operating points. The dimensionless velocity profiles both the measured and simulated time-averaged axial and tangential velocity are presented and compared to validate numerical simulation method at different loads. The tangential velocity and vortex ropes visualization at various loads are used to analyze that how the operating parameters of flowrates and heads have effects on velocity profiles and swirl flows inside draft tube. The measured instantaneous tangential velocity is used to determine the dominating frequency of rotating vortex ropes and verify the 3D unsteady flows simulations at part loads. The validated numerical simulation method further offers the possibility to assess performance in optimization design of a pump-turbine.

2. Experimental Set Up and LDV Measurement

2.1 Test Rig

The experimental study was undertaken on a scaled Francis pump-turbine model with runner outlet diameter of 260mm. The distributor of the model is equipped with 16 guide vanes and a runner with 5 splitters and 5 full length blades. The model was mounted in a high precision commercial hydraulic machinery test stand with a closed-loop system at Hydraulic Laboratory of DFEM Co. Ltd. in China. The systematic errors of the test stand is within ±0.25% according to IEC60193 standard [10]. Due to its high demand for optical access of LDV measurement, an optical interface for measurements were carefully designed in the draft tube by taking into account the internal geometry of the model, local optical distortions and perspective effects from the curved surface. For the velocity measurements, a LDV system from TSI Co. Ltd. was used with a NC controlled traverse system which equipped with the servomotor to accurately move and position the probe. The model turbine setup and the LDV probe mounted on the traverse system are shown in figure 1.

Figure 1. The model turbine setup and the LDV probe

2.2 LDV setup and calibrations

The TSI LDV system with 5W Solid State lasers to generate high quality Doppler signals, which consisted of laser unit (type LA70-5)， multicolor beam separator(type FBL-3 Fiberlight™), signal processor(type FSA4000-3P), photoelectric detector module(type PDM1000-3P), transmitting laser probe(type TM250) and FlowSizer® software, was used to measure the axial and tangential velocity components of flows inside the draft tube. The range of velocity measurements is within-150m/s~+1000m/s, velocity accuracy< 0.2%, and the repeatability of individual velocity measurements has been shown to be better than 0.05% for this LDV system. To evaluate the accuracy of the measured velocity components with this experimental setup, the flowrates measured with LDV are calculated by integrated the axial velocity components with the measurement plane, the flowrates deviations between the integral of LDV measured axial velocity profiles and the measured by the installed high precision electromagnetic flowmeter are within ±1.85% for all the measuring points. The larger deviations at part load compared to BEP and full load is attributed to presence of the rotating vortex rope. An encoder installed on the main shaft allowed the measured velocity components to be phase-resolved with respect to the runner frequency. As Doppler velocity measurement method is based on measuring the frequency of the laser radiation scattered of moving subject, spherical particles in hollow glass spheres, are added to the water as flow tracers. Its relative density is about 1.008 against the water and the average size of 10μm glass spheres allow these particles to accurately follow the water flow inside the draft tube. The measurement time per point is not less than 300 seconds, assuring a sufficiently high number of vortex rope revolutions. The count number of all points is at least

30000, up to 50000 counts, which makes the total averaged value highly accurate. As there has great difference of the laser speed in water, air and Plexiglas, the actual position of the optical axis of LDV is required to be calibrated in-situ. After calibration in-situ, the transform ratio of this optical access is 1.33, which means it is necessary to increase coordinate in the water 1.33 times than actual measured coordinate in the air while LDV measuring.

3. LDV measurements

3.1 Measurement positions

As shown in figure 2, LDV measurements were performed on the section located D_2=260mm in axially below the centerline of distributor. The velocity profiles were measured at 29 radial points which at the step-length of 0.05R from r_a=0 to 0.9R and 0.01R from r_a=0.9R to 1.0R (R=138.6mm). To position the laser probe along radial position of the measurement path, the NC controlled traverse system is constructed and the radial coordinate of laser probe is positioned automatically by the linear traverse according to the setup in FLOWSIZER™.

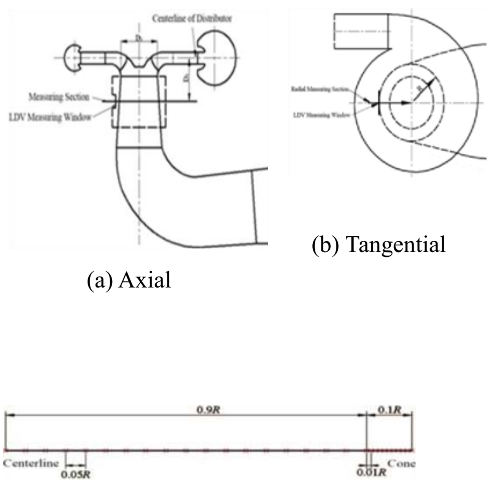

(a) Axial

(b) Tangential

(c) layout of measured points in radius

Figure 2. Measurement positions

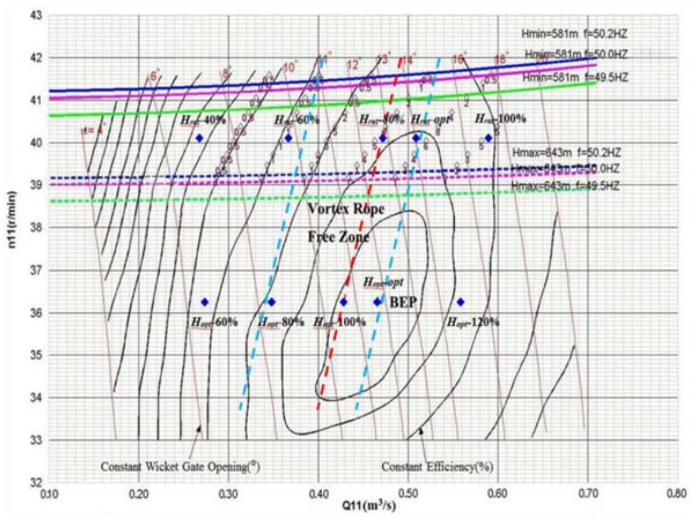

Figure3. Measured Operating points labelled at the hill diagram（n_{ED} =0.005322 n_{11}, Q_{ED}= 0.31933 Q_{11} ）(n_{11}: unit speed, Q_{11}: unit discharge）

3.2 Measured operating points

LDV measurements were carried out at non-cavitation operating conditions. Dimensionless parameters n_{ED} and Q_{ED}, which are defined by equation (1), are used to describe the turbine operating points. 10 measured operating points were taken at closer to the speed factor n_{ED}=0.21 and 0.19 at turbine mode for different loads corresponding to these operating points are labelled in figure 3 and their detailed parameters are presented in table1 and 2. For pump mode, measurements were taken for operating at H_{min}-Q_{max} and H_{max}-Q_{min}. The absolute values of test head, flow rate and runner's rotating speed were therefore adjusted according to table1 and 2 while the speed factor n_{ED} were kept constant approximately (Notes: *opt* and *rat* are subscripts to respectively represent the optimum head and the rated head) and the Relative Power were adjusted to the corresponding Operating point.

$$n_{ED} = n.D / \sqrt{gH}, \qquad Q_{ED} = Q / D^2 \sqrt{gH} \tag{1}$$

Where: n is the rotating speed in *r/s*; D is the diameter of the runner in *m*; g is the local gravitational acceleration m/s^2; H is the measured head in *m*; Q is the measured discharge in *m*^{3}*/s*.

Table 1. Operating conditions were measured closer to n_{ED} =0.21 at turbine mode

Relative Power P/P_r(%)	Q (m^3/s)	Runner speed n (*rpm*)	Test head H (m)	OP No.
40	0.10362	939.87	36.94	Hrat-40% P_r
60	0.14334	925.87	35.52	Hrat-60% P_r
80	0.18581	919.86	35.04	Hrat-80% P_r
100	0.23465	919.85	35.21	Hrat-100% P_r
Opt *(around BEP)*	0.19984	919.86	35.60	Hrat-opt

Table 2. Operating conditions were measured closer to n_{ED}=0.19 at turbine mode

Relative Power P/P_r(%)	Q (m^3/s)	Runner speed n (*rpm*)	Test head H (m)	OP No.
60	0.10508	839.90	38.15	Hopt-40% P_r
80	0.13541	825.01	36.93	Hopt-60% P_r
100	0.16574	821.94	35.81	Hopt-80% P_r
Opt *(BEP)*	0.18220	809.93	35.02	Hopt-Opt
120%Q_{Opt}	0.21875	809.78	34.98	Hopt-120% Q_{opt}

3.3 Results of LDV measurements

To describe the velocity in draft tube, the positive axial velocity is defined in the stream-wise direction and the tangential velocity is positive in the runner rotational direction for turbine mode, and the velocity is negative in the runner rotational direction for pump mode. All the spatial coordinates of measured position are normalized with the draft tube radius R from the center to cone wall on the measured section as shown in figure 2c). The velocity components are made dimensionless coefficients using the following equations for turbine mode.

$$K_{cu} = C_u / \sqrt{2gH}, \qquad K_{cm} = C_m / \sqrt{2gH} \tag{2}$$

Where: K_{cu}, K_{cm} are the tangential and axial velocity coefficients respectively; C_u, C_m are the tangential and axial velocity in *m/s*; H is the measured head in *m*.

3.3.1 Time-averaged velocity and vortex rope

The time-averaged velocity distribution on the section of draft tube inlet reflects the runner downstream flow, which can be used to classify the flow pattern and analyze the hydraulic stability of the operating condition. If K_{cm}<0, there exists backwards flows inside draft tube cone, and if K_{cu}<0, there exists vortex rotating with the reversed direction of runner's rotation, and K_{cu}>0, vortex rotating with the direction of runner's rotating. To better understand the flow pattern classification based on the measured velocity components distribution, the vortex rope visualization at the corresponding operating condition was carried out while measuring. As shown in figure 2(a), the measurement plane is near to the draft tube inlet. To show the time-averaged velocity distribution, the tangential and axial velocity coefficients are calculated based on equation (2) and plotted along radial measurement point's position.

(1) Operating under the rated head

Figure 4 shows the measured tangential and axial velocity coefficients when operates closer to the speed factor n_{ED}=0.21 corresponding to the rated head H=600m of prototype at turbine mode. At Hrat-40%Pr operating point, the velocity distribution is featured with Kcm<0 and Kcu≈0 within r/R=0~0.5, which indicates a stronger backflow and column vortex due to the operation at deep part load. As shown in figure 5(a), due to the emergence of vortex breakdown, the time-averaged velocity profiles are completely different than those for the BEP and higher load. At Hrat-60%Pr operating point, a vortex rope was observed as shown in figure 5(b), as the tangential velocity distribution is featured with Kcm>0 and Kcu>0 within r/R=0.0~0.95 but Kcu≈0 within r/R=0~0.2, its velocity distributions indicate that the vortex rope rotates in the same direction as the runner. At Hrat-80%Pr operating point, the axial velocity is almost evenly distributed within r/R=0.1~0.95 while decreases near the wall due to the boundary effect, and the tangential velocity slightly and linearly increases from Kcu≈0.0 to Kcu≈0.03 within r/R=0.0~0.1, and then almost linearly decreases from Kcu≈0.03 to Kcu≈-0.03 within r/R=0.1~1.0 due to design of blade trailing edges. As shown in figure 3, this operating point is closer to BEP and there is no visible vortex for the flow leaving the runner as shown in Figure 5(c). At Hrat-opt operating points, it can be clearly seen from the measured velocity profiles that small size straight vortex rope exists in center region of draft tube cone as Kcu linearly increases from -0.01 to 0.09 within r/R=0.0~0.17. Observation as shown in figure 5(d) also confirms this phenomenon. At Hrat-100%Pr operating point, a contra-rotating flow region is observed in the mean tangential velocity component and vortex rope observation as shown in figure 5(e). The tangential velocity coefficient Kcu<0 within r/R=0.0~1.0 and the minimum value appears at the position near r/R=0.42, and its distribution indicates that the vortex rope rotates in counter-wise direction to the runner rotating.

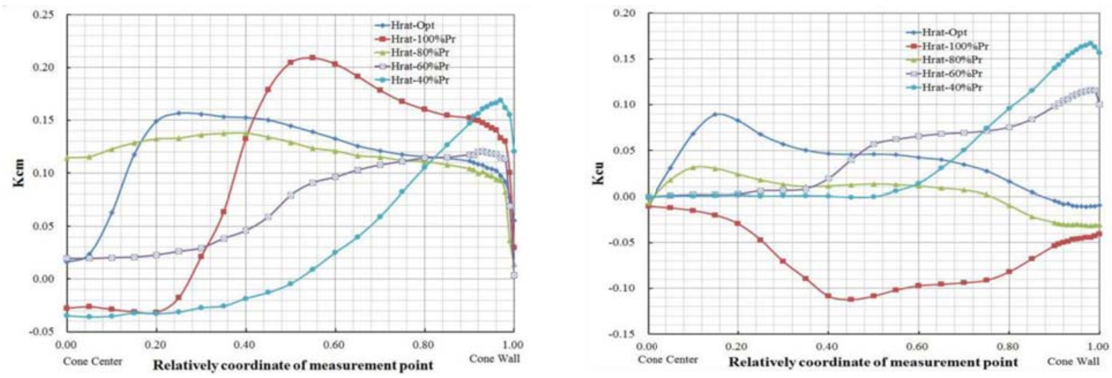

(a) axial velocity coefficients (b) tangential velocity coefficients

Figure 4. Velocity coefficients at 5 operating points closer to the speed factor n_{ED}=0.21

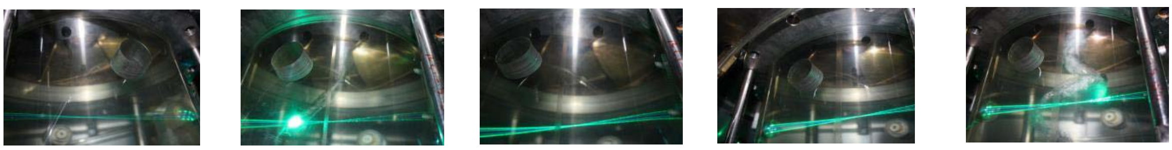

(a) *Hrat*-40%*Pr* **(b)** *Hrat*-60%*Pr* **(c)** *Hrat*-80%*Pr* **(d)** *Hrat-opt* **(e)** *Hrat*-100%*Pr*

Figure 5. Vortex ropes visualization at operating closer to speed factor n_{ED}=0.21

IOP Conf. Series: Earth and Environmental Science **240** (2019) 072044 doi:10.1088/1755-1315/240/7/072044

(2) Operating under the optimum head

Figure 6 shows the measured tangential and axial velocity coefficients when operates closer to the speed factor n_{ED}=0.19 corresponding to the optimum head H=750m of prototype at turbine mode. At Hopt-60%Pr operating point, the velocity distribution is featured with *Kcm*<0 and *Kcu*≈0 within *r/R*=0~0.45. This means stronger backflow and intensive swirl so that the stagnation point locates near the inlet of draft tube, therefore a single stable vortex rope is observed as shown in figure 7(a), which is typical vortex rope for a high head turbine operating at part load. At Hopt-80%Pr operating point, the axial velocity is almost evenly distributed within *r/R*=0.28~0.95 while decreases near the wall due to the boundary effect, and the tangential velocity linearly increase from *Kcu*≈0.0 to *Kcu*≈0.10 within *r/R*=0.0~0.95 along the radius. At Hopt-100% Pr and Hopt-opt *(BEP)* operating points, their velocity profiles are very similar as Hopt-100% Pr is close to *BEP* as shown in figure 3. It can be clearly seen from the measured velocity profiles that small size vortex rope exists in center region of draft tube cone. Observation as shown in figure 7(c) and (d) also confirms this phenomenon. At Hopt-120% Q_{opt} operating point, the tangential velocity is negative and the minimum value appears at the position near *r/R*=0.45. This indicates that there exists a vortex rope rotating in opposite direction to the runner rotating. This flow pattern, mainly due to operation at high load and very high head, can also be clearly observed in figure 7(e).

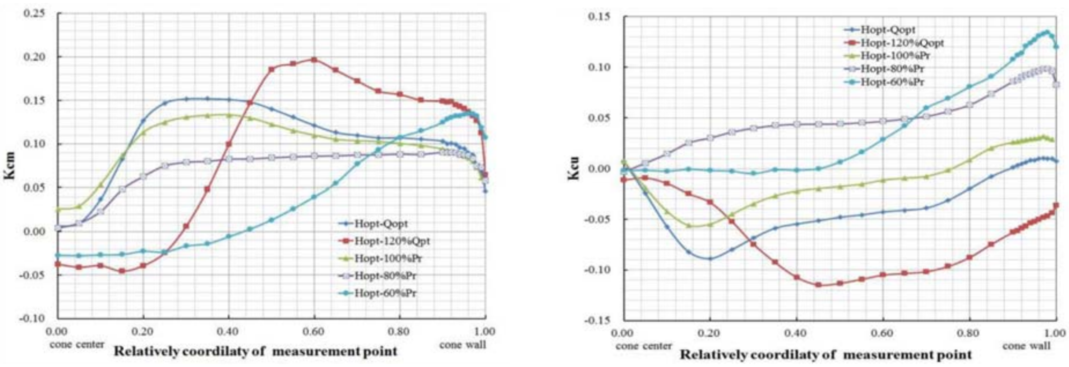

(a) axial velocity coefficients

(b) tangential velocity coefficients

Figure 6. Velocity coefficients at 5 operating points closer to the speed factor n_{ED}=0.19

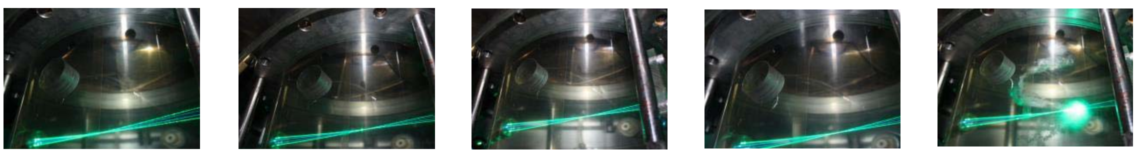

(a) H_{opt}-60%*Pr* **(b)** H_{opt}-80%*Pr* **(c)** H_{opt}-100%*Pr* **(d)** $H_{opt-opt}$ **(e)** H_{opt}-120% Q_{Opt}

Figure 7. Vortex ropes visualization at operating closer to speed factor n_{ED}=0.19

(3) Operating under pump mode

Figure 8 shows the measured tangential and axial velocity components at pump mode while operating at (H_{min}-Q_{max}) and (H_{min}-Q_{min}). At all the measured operating conditions, the axial velocity is almost constant distribution and the values depend on the discharge and the tangential velocity close to zero ranging from r/R =0~0.95 on the measurement plane, but sharply decrease close to the cone wall due to the boundary layer or may be related to the tip clearance of runner's band.

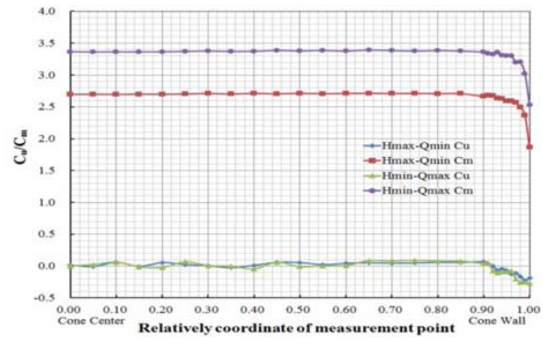

Figure 8. Tangential and axial velocity at pump mode

3.3.2 Instantaneous tangential velocity and fluctuation characteristics of vortex rope

The measured velocity fluctuations can be further used to validate the characteristics of the vortex rope. Taking operating point at the part load of 60%P_r (Hrat-60%P_r) for example, the measured tangential velocity fluctuations of 12 measuring positions from r/R =0 to 0.55 within 2 seconds were recorded and fitted to obtain the time domain of the measured tangential velocity, and figure 9 shows the time domain for measuring positions at r/R =0.3 and 0.5, and figure 10 shows the frequency domain for measuring positions at r/R =0.3 and 0.5 after FFT was carried out.

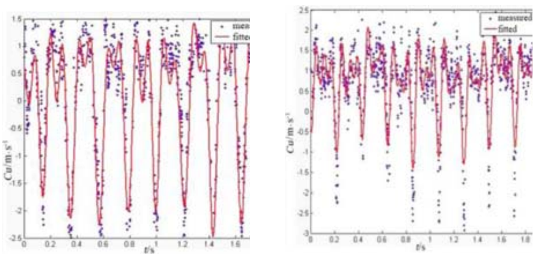

(a) $r/R=0.3$ (b) r/R =0.5

Figure9. Tangentail velocity within 2s at Hrat-60%P_r

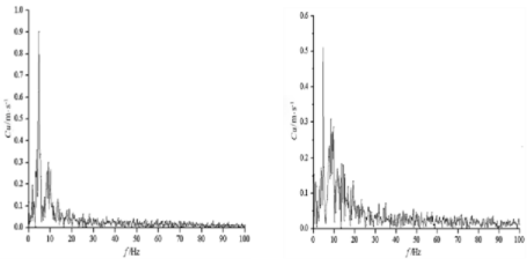

(a) $r/R=0.3$ (b) r/R =0.5

Figure 10. Fluctuations frequency at Hrat-60%P_r

The main frequency of the measured tangential velocity fluctuations at 12 measuring positions from r/R =0 to 0.55 (Due to the vortex rope was observed within r/R <0.4 at this operating point) are listed in table 3, the arithmetic mean of the main frequency for 12 measuring positions is 4.65Hz, which is 0.28 times of rotating frequency of turbine runner at this operating point.

Table 3. Main frequency of instantaneous tangential velocity fluctuations for 12 measuring positions

position	0	0.05R	0.10 R	0.15 R	0.20 R	0.25 R
freq/Hz	4.49	4.72	4.73	4.78	4.61	4.57
position	0.30R	0.35 R	0.40 R	0.45 R	0.50 R	0.55 R
freq/Hz	4.71	4.53	4.80	4.72	4.61	4.57

4. Numerical Simulation Setup

The numerical simulations were carried out by using the commercial flow solver ANSYS CFX applied to the complete pump turbine model with all its hydraulic components. The calculations were conducted in a coupled manner, i.e. considering all the turbine components and interfaces between them, as long as the dynamic effects in the flow through the turbine arise from the interaction between its components, caused by the rotating runner and the stationary parts.

The unstructured mesh in the completed pump turbine model was prepared using ICEM CFD, and was divided into 3 domains: the spiral casing with distributor, runner, and draft tube. The mesh was independently created in all domains. Different computational mesh densities were tested and optimized to deliver accurate results with acceptable computation times. The final computational mesh counted with around 18 million cells and part of it can be seen in figure 11. As the inflow boundary condition the volume flow was prescribed together with 5% turbulence intensity, and at outlet a reference integral pressure level was prescribed and allowed any eventual backflow.

(a) geometric model (b) mesh (c) vortex rope at Hopt-60%Pr

Figure 11. Complete pump turbine geometric model, mesh and simulated vortex rope

Considering the turbulence modelling, the unsteady RANS model introduced, as expected, excessive artificial dissipation in the flow simulation and turned out to be unable to reproduce the highly transient effects in the turbine draft tube. Therefore, adequate and more sophisticated turbulence models had to be employed. The scale adaptive simulation (SAS) [11] was chosen to simulate the flows through turbine as it was already repeatedly and successfully employed in the past few years for the numerical simulation of the transient fluid flow with accurate results. Frozen rotor and transient rotor-stator interface were applied to steady and unsteady flow simulation respectively in in the completed pump turbine model.

5. Numerical results in comparison with experimental data

To validate the simulated results, 4 operating points including the over-load (Hopt-opt), full-load (Hopt-100%Pr), part load (Hopt-60%Pr) and deep part load (Hopt-40%Pr) under operating at the optimum head are selected to compare with experimental data. These different operating conditions constituted an interesting benchmark for the prediction capability of the numerical simulation model. They counted with different flow effects taking place in the hydraulic turbine, rotor-stator interaction, rotating draft tube vortex rope and runner channel vortex.

The comparison of the simulated tangential and axial velocity coefficients with the measured at 4 selected operating points are shown in figure 12. At deep part load (Hopt-40%Pr), there are larger discrepancies between the measured and CFD computed in the axial velocity components ranging from r/R=0 to 0.45 as the stronger

IOP Conf. Series: Earth and Environmental Science **240** (2019) 072044 doi:10.1088/1755-1315/240/7/072044

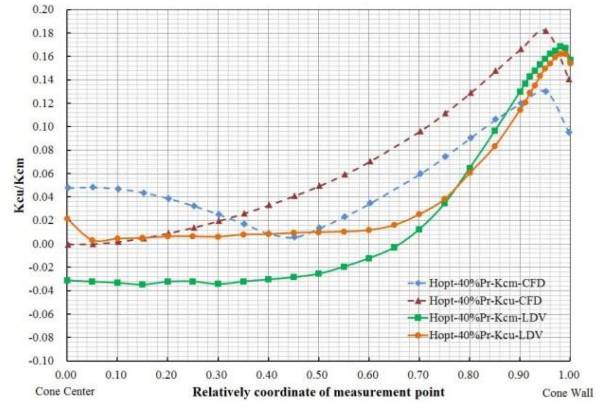

(a) Hopt-40%P_r

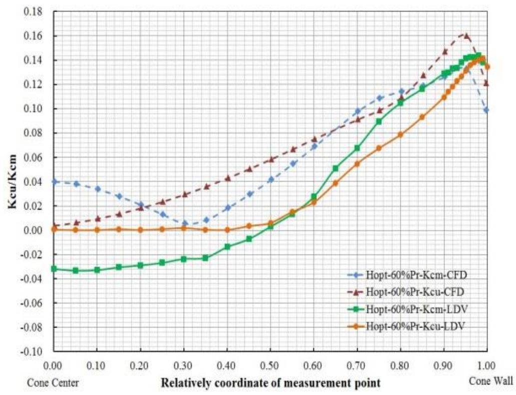

(b) Hopt-60%P_r

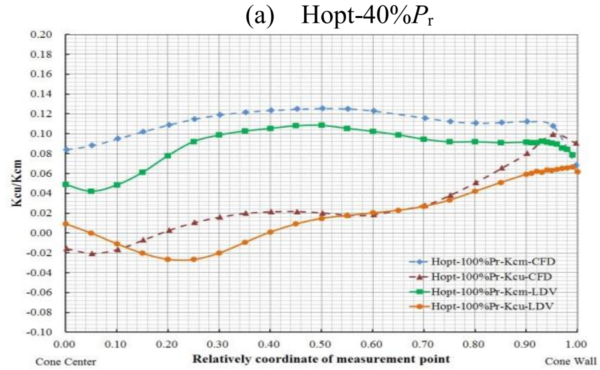

(c) Hopt-100%P_r

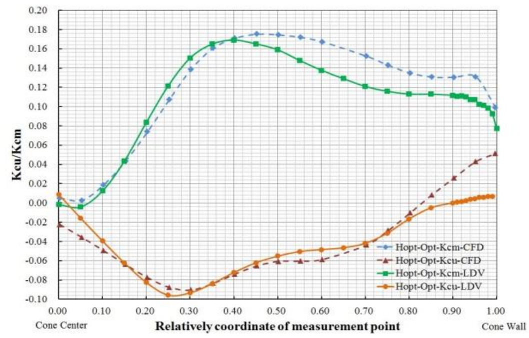

(d) Hopt-opt

Figure 12. The comparison of the simulated with the measured tangential and axial velocity coefficients

backward flows observed and the largest discrepancies is close to the draft tube axis, but their trend lines agree well in ranging from r/R=0.45 to 0.9. The measured and computed tangential velocity agree well in ranging from r/R=0 to 0.25 and their profiles agree well only in trend line ranging from r/R=0.25 to 0.95 but the value is over-estimated due to the vortex rope as shown in figure 12(a). At part load (Hopt-60%Pr), their profiles are similar to the Hopt-40%Pr as shown in figure 12(b). At full load (Hopt-100%Pr), as shown in figure 12(c), it shows very good agreement for the axial velocity apart in the ranging from r/R=0 to 0.2. The measured and CFD computed tangential velocity agree well in ranging from r/R=0.45 to 0.8 and the larger discrepancies in ranging from r/R=0. to 0.45, and profile's tendency agree well in ranging from r/R=0.8 to 0.95 but its value is over-estimated.

Analysis shows that axial velocity profiles are much better predicted than the tangential ones at full-load (Hopt-100%Pr) and over-load (Hopt-opt), while in the wall region the inaccuracy between measurements and computations is probably caused by the near wall modelling, the significant variation in the central region is attributed to inaccuracy of both LDV measurements and turbulence models in flow computation. Figure 11(c) shows the simulated vortex rope at Hopt-60%Pr, and it is similar to the observed in model test as shown in figure 7.

6. Conclusions

Flows in the draft tube of a high-head Francis pump-turbine model at cavitation-free operating conditions were preliminarily investigated with LDV measurements and CFD simulations, the investigated operating points cover the turbine's loads ranging from 40-120% rated power at the speed factor n_{ED}=0.21 and 0.19. It has shown that:

（1） The measured velocity profiles are well-distributed and the measured results indicate a well-functioning turbine when operating closer to BEP. However, when operating at lower than 60% rated power, the velocity profiles are distorted and vortex breakdown occurrences which creates a recirculation region covering more than half of the cone radius, and it will significantly affects the velocity measuring accuracy.

（2） Comparison of the measurement and simulation results shows rather good agreement in the zones around BEP but clear discrepancies at deep part loads. The velocity components prediction accuracy of the numerical simulations depends on the operating zones. The measured low frequency pressure pulsations are quite similar to the predicted by the simulations.

（3） Although the measured velocity data with 2D LDV can be provided as a reference for validation data for numerical simulation in optimization design, flow visualization or joint LDV and PIV measurements should be used for further investigations of 3D complex structures inside the draft tube at unsteady and cavitating operating conditions.

Acknowledgments
The research was supported by the Major Research Plan of Sci.&Tech. of Sichuan Province in China (Grant No.2017JY0047, 2017GZ0053, 2017NZ0031), and partially supported by Natural Science Foundation of China under the Grant No.51379179 and the Foundation of Key Laboratory of Fluid and Power Machinery (Xihua University), Ministry of Education of China. Their supports are greatly appreciated.

References

[1] U Jese, R Fortes-Patella and S Antheaume 2016 High head pump-turbine: Pumping mode numerical simulations with a cavitation model for off-design conditions *Proceeding of the 28th IAHR Symposium on Hydraulic Machinery and System* Grenoble France.
[2] Krappel T, Riedelbauch S, Jester-Zuerker R, Jung A, Flurl B, Unger F, Galpin P. 2016, Turbulence Resolving Flow Simulations of a Francis Turbine in Part Load using Highly Parallel CFD Simulations, *Proceeding of the 28th IAHR Symposium on Hydraulic Machinery and System*, Grenoble, France.
[3] X Zhang, R Burgstaller, X D Lai 2016 Experimental and Numerical Analysis of Performance Discontinuity of a Pump-Turbine under Pumping Mode *Proceeding of the 28th IAHR Symposium on Hydraulic Machinery and System* Grenoble France.
[4] Trivedi C, Cervantes M, Gandhi B, Dahlhaug O 2013 Experimental and Numerical Studies for a High Head Francis Turbine at Several Operating Points *Journal of Fluids Engineering* vol 135(11).
[5] Gentner Ch 2012 Numerical and experimental analysis of instability phenomena in pump-turbines *Proceeding of the 26th IAHR Symposium on Hydraulic Machinery and System* Beijing China.
[6] Ciocan G D, Iliescu M S, Vu T C, Nennemann B, Avellan F 2007 Experimental Study and Numerical Simulation of the Flindt Draft Tube Rotating Vortex J *Fluids Eng* Vol129 pp 146-158.
[7] Chirag Trivedi, Michel J. Cervantes and Ole G. Dahlhaug 2016 Experimental and Numerical Studies of a High-Head Francis Turbine: A Review of the Francis-99 Test Case *Energies* Vol74 pp 1-24.
[8] L R J sundstrom, K Amiri, and C Bergan 2014 LDA measurements in the Franci-99 draft tube cone *Proceeding of the 27th IAHR Symposium on Hydraulic Machinery and System* Montreal Canada.
[9] M Guggenberger, F Senn, J Schiffer, H Jaberg 2014 Experimental investigation of the turbine instability of a pump-turbine during synchronization *Proceeding of the 27th IAHR Symposium on Hydraulic Machinery and System* Montreal Canada.
[10] IEC60193 Hydraulic turbines storage pumps and pump-turbines – Model acceptance tests Second edition 1999.
[11] Menter F R and Egorov Y 2010 The Scale-Adaptive Simulation Method for Unsteady Turbulent Flow Predictions *Part 1 Theory and Model Description Journal of Flow Turbulence and Combustion* Vol85(1) pp 113-138.